



Discovery of Sulfonamidebenzamides as Selective Apoptotic CHOP Pathway Activators of the Unfolded Protein Response

Daniel P. Flaherty,[†] Justin R. Miller,[‡] Danielle M. Garshott,[‡] Michael Hedrick,[§] Palak Gosalia,[§] Yujie Li,[§] Monika Milewski,[§] Eliot Sugarman,^{||} Stefan Vasile,^{||} Sumeet Salaniwal,[§] Ying Su,[§] Layton H. Smith,^{||} Thomas D. Y. Chung,[§] Anthony B. Pinkerton,[§] Jeffrey Aubé,[†] Michael U. Callaghan,[‡] Jennifer E. Golden,^{*,†} Andrew M. Fribley,^{*,‡} and Randal J. Kaufman^{*,†}

[†]Delbert M. Shankel Structural Biology Center, University of Kansas Specialized Chemistry Center, 2034 Becker Drive, Lawrence, Kansas 66047, United States

[‡]Carmen and Ann Adams Department of Pediatrics, Division of Hematology and Oncology, and the Karmanos Cancer Institute Molecular Therapeutics Group, Wayne State University, 2228 Elliman Building, 421 East Canfield, Detroit, Michigan 48201, United States

[§]Conrad Prebys Center for Chemical Genomics, Sanford-Burnham Medical Research Institute, La Jolla, California 92037, United States

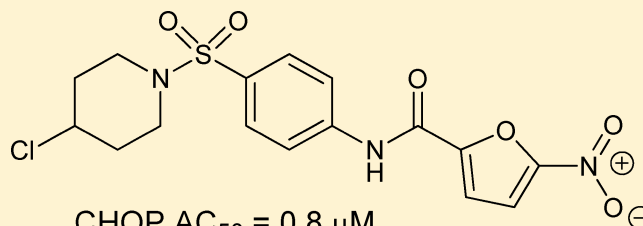
^{||}Conrad Prebys Center for Chemical Genomics, Sanford-Burnham Medical Research Institute at Lake Nona, Orlando, Florida 32827, United States

[⊥]Program in Degenerative Disease Research, Sanford-Burnham Medical Research Institute, 10901 North Torrey Pines Road, La Jolla, California 92037, United States

S Supporting Information

ABSTRACT: Cellular proteins that fail to fold properly result in inactive or dysfunctional proteins that can have toxic functions. The unfolded protein response (UPR) is a two-tiered cellular mechanism initiated by eukaryotic cells that have accumulated misfolded proteins within the endoplasmic reticulum (ER). An adaptive pathway facilitates the clearance of the undesired proteins; however, if overwhelmed, cells trigger apoptosis by upregulating transcription factors such as C/EBP-homologous protein (CHOP). A high throughput screen was performed directed at identifying compounds that selectively upregulate the apoptotic CHOP pathway while avoiding adaptive signaling cascades, resulting in a sulfonamidebenzamide chemotype that was optimized. These efforts produced a potent and selective CHOP inducer (AC_{50} = 0.8 μ M; XBP1 > 80 μ M), which was efficacious in both mouse embryonic fibroblast cells and a human oral squamous cell cancer cell line, and demonstrated antiproliferative effects for multiple cancer cell lines in the NCI-60 panel.

KEYWORDS: CHOP activator, UPR modulator, UPR apoptotic pathway activator, anticancer



CHOP AC_{50} = 0.8 μ M
XBP1 AC_{50} > 80 μ M

It has been estimated that nearly one-third of the human genome encodes proteins that enter the secretory pathway en route to their final destination. Proteins that are secreted, cell membrane bound (including receptors), or function in a lysosome are folded and post-translationally modified in the endoplasmic reticulum (ER).^{1–3} Homeostatic maintenance within the ER is imperative for proper manufacture and modification of essential proteins. Disruption of this process by pharmacological insults that perturb N-linked glycosylation, disulfide bond formation or calcium or redox status can lead to an accumulation of misfolded and nonfunctional proteins within the organelle, a condition known as ER stress.^{2,4} The unfolded protein response (UPR) is a coordinated attempt by the cell to either restore protein folding or induce apoptosis if homeostasis cannot be restored.² The accumulation of

misfolded proteins immediately triggers an adaptive response whereby the ER transmembrane protein inositol-requiring enzyme, 1 α (IRE1 α), splices X-box binding protein 1 (XBP1) mRNA, unleashing its potential as a transcription factor, in an effort to enhance protein folding and degradation of misfolded proteins.^{5,6} Simultaneously, another ER transmembrane kinase, RNA-like endoplasmic reticulum kinase (PERK), is activated to cause an immediate transient attenuation of general mRNA translation. If productive folding cannot be restored and the burden of misfolded proteins persists, accumulation of activating transcription factor 4 (ATF4) and C/EBP-homolo-

Received: August 1, 2014

Accepted: October 29, 2014

Published: October 29, 2014



gous protein (CHOP) leads to programmed cell death by upregulating apoptotic genes and modulating the reinitiation of protein synthesis.^{7–11} Indeed, recent studies suggest that CHOP acts as a tumor suppressor gene.¹² It has been shown that ER stress and the UPR contribute to neurodegenerative¹³ and inflammatory¹⁴ diseases, metabolic disorders,¹⁵ diabetes,¹⁶ and cancer;¹⁷ modulating the UPR with chemical probes as a means of addressing these conditions, especially cancer, has been studied by our group and others.^{18–23}

Previously reported UPR modulators include promoters of the UPR adaptation mechanisms as well as those that inhibit UPR pro-survival signaling.²⁴ Compounds of the latter group operate by modulating one or more components within the apoptotic pathway, and many of these agents have been pursued as cancer therapeutics. Sorafenib **1** is an FDA-approved drug for certain kidney and liver cancers that is known to inhibit multiple receptor tyrosine kinases and serine/threonine kinases (Figure 1).^{25,26} More recently, the compound has been

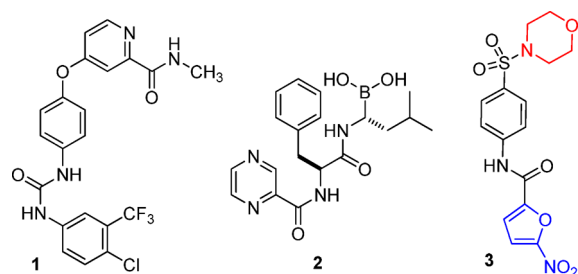


Figure 1. UPR activators sorafenib **1**, bortezomib **2**, and sulfonamidebenzamide hit **3** with colored regions of SAR focus.

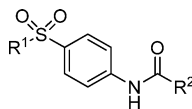
identified as an inducer of the UPR through inhibition of the p97 ATPase, a cellular enzyme that regulates protein degradation in the ER.²⁷ Other p97 ATPase inhibitors have also been reported,^{28,29} along with inhibitors of the molecular chaperone, Hsp90.³⁰ Lastly, bortezomib (Velcade) **2** is a dipeptide boronic acid derivative that is FDA-approved for multiple myeloma. While bortezomib **2** was found to effectively inhibit the proteasome, thereby activating UPR-dependent apoptotic cellular mechanisms,^{31–34} the compound has been shown to also attenuate adaptive response cascades in human multiple myeloma cells and select for cells that have reduced expression of secretory proteins.^{35,36} While none of these agents were derived from efforts to identify UPR-focused targets, they were all found to directly or indirectly modulate UPR activity. We hypothesized that a high throughput screen (HTS) aimed at identifying compounds that broadly function as pro-apoptotic UPR stimulants might provide novel starting scaffolds for further development.^{23,37} Conceptually, small molecules that selectively induced the apoptotic PERK-CHOP pathway *independently* of the IRE1 α -XBP1 pathway were sought to properly interrogate the utility of a selective CHOP activator.

This pursuit was initiated by performing an HTS of 331,676 Molecular Libraries Small Molecule Repository (MLSMR) compounds as part of the NIH Molecular Libraries Probe Production Centers Network (MLPCN).³⁸ The HTS assay assessed compounds at 10 μ M for 6–8 h in Chinese hamster ovary (CHO) K1 cells containing luciferase constructs that individually reported on *Chop* activation or *Xbp1* splicing.³⁹ Hit compounds were defined as those that generated $\geq 40\%$ luciferase in the CHOP-luc cells compared to tunicamycin

(Tm)-treated positive controls. After retesting these at the same concentration, compounds displaying $\geq 32\%$ of Tm-induced luciferase were subjected separately to dose–response assays with CHO-CHOP-luc cells or CHO-XBP1-luc cells to remove compounds that nonselectively activated the UPR.⁴⁰ Several scaffolds were identified from this effort; however, sulfonamidebenzamide **3** was one of the most promising, exhibiting a CHOP $AC_{50} = 1.9 \mu$ M and an XBP1 $AC_{50} > 80 \mu$ M (Figure 1). Analogues of **3** were generated to establish structure–activity relationships (SAR) around the scaffold, optimize the activity, and further characterize this structural series in relevant cancer cell lines (Table 1).

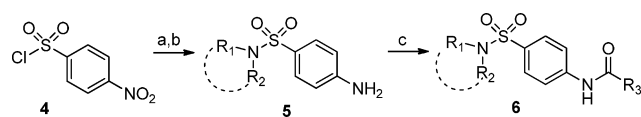
The majority of analogues was synthesized by coupling 4-nitrobenzenesulfonyl chloride **4** with various cyclic amines to afford *para*-nitrophenylsulfonamide intermediates (Scheme 1). The nitro group was subsequently reduced with Raney nickel

Table 1. CHOP and XBP1 Activity for Structural Changes in **3**



compd	R ¹	R ²	UPR CHOP $AC_{50} \pm SEM$ (μ M) ^a	UPR XBP1 AC_{50} (μ M) ^a
3	N-morpholine	5-NO ₂ -furan	1.9 \pm 0.4	>80
7	3,5-(CH ₃) ₂ -N-morpholine	5-NO ₂ -furan	1.4 \pm 0.4	>80
8	N-piperazine	5-NO ₂ -furan	26.4 \pm 1.5	>80
9	4-hydroxy-N-piperidine	5-NO ₂ -furan	2.0 \pm 0.4	>80
10	N-piperidine	5-NO ₂ -furan	1.2 \pm 0.2	>80
11	4-F-N-piperidine	5-NO ₂ -furan	0.6 \pm 0.1	>80
12	4-Cl-N-piperidine	5-NO ₂ -furan	0.8 \pm 0.04	>80
13	4-CH ₃ -N-piperidine	5-NO ₂ -furan	0.7 \pm 0.1	>80
14	4-(CH ₃) ₂ -N-piperidine	5-NO ₂ -furan	0.6 \pm 0.1	>80
15	4- <i>tert</i> -butyl-N-piperidine	5-NO ₂ -furan	0.7 \pm 0.1	>80
16	N-3-azaspiro [5.5]undecane	5-NO ₂ -furan	0.7 \pm 0.1	>80
17	N-pyrrolidine	5-NO ₂ -furan	0.8 \pm 0.03	>80
18	phenyl	5-NO ₂ -furan	1.1 \pm 0.2	>80
19	4-pyran	5-NO ₂ -furan	1.2 \pm 0.2	>80
20	cyclohexyl	5-NO ₂ -furan	0.7 \pm 0.04	>80
21	N-morpholine	5-NO ₂ -2-thiophene	13.5 \pm 0.5	>80
22	N-morpholine	2-thiophene	>80	>80
23	N-morpholine	phenyl	>80	>80
24	N-morpholine	4-NO ₂ -phenyl	>80	>80
25	4-(CH ₃) ₂ -N-piperidine	3-NO ₂ -phenyl	>80	>80
26	4-(CH ₃) ₂ -N-piperidine	1-CH ₃ -5-NO ₂ -2-imidazole	>80	>80
27	N-morpholine	2-furan	>80	>80
28	N-morpholine	5-CH ₃ -furan	>80	>80
29	N-morpholine	5-Br-furan	>80	>80
30	4-(CH ₃) ₂ -N-piperidine	5-CF ₃ -furan	>80	>80

^aData were averaged from $n \geq 4$ experiments.

Scheme 1. General Synthesis of the Sulfonamidebenzamide Scaffold^a

^aReagents and conditions: (a) amine, pyridine, THF, 60 °C, 20 min, 38–98%; (b) Raney Ni, NaBH₄, CH₃OH/CH₂Cl₂, 0 °C, 30 min, 54–98%; (c) acyl chloride, acetonitrile, 150 °C, μ W, 20 min, 38–86%.

and NaBH₄ to unmask anilines **5**, which were then treated with acyl chlorides to deliver desired analogues **6**. For several derivatives, the requisite aniline **5** was commercially available. Analogue **19** was prepared from an S_N2 displacement of 4-bromotetrahydropyran with 4-nitrothiophenol, followed by subsequent oxidation of the thioether. Analogue **20** required an adapted S_NAr route,⁴¹ followed by oxidation of the resulting thioether to the sulfone, thus affording a 4-nitrophenylsulfone intermediate. These 4-nitrophenyl intermediates were transformed uneventfully to their corresponding products as shown in Scheme 1.

Structural modifications initially focused on the morpholine ring (red region of **3**, Figure 1). Compounds bearing morpholine ether oxygen alternatives were prepared to survey the impact of hydrogen bonding, basicity, and lipophilicity at that structural position on CHOP activation (Table 1). The incorporation of the more basic, NH-donor of piperazine **8** was not tolerated, resulting in a nearly 14-fold loss of activity. The nonbasic phenolic analogue **9** activated CHOP on par with activity observed with hit **3**. However, replacement of polar functionality at this 4-position with lipophilic components resulted in the greatest improvement in CHOP activation. Better activity was observed with 4-halogenated analogues **11** and **12** (0.6 and 0.8 μ M, respectively) and 4-methylated variants **13** and **14** (0.7 and 0.6 μ M, respectively). In fact, a range of lipophilic substitution was tolerated, including a *tert*-butyl group and a spirocyclohexyl appendage (analogues **15** and **16**). Replacement of the sulfonamide linkage with a sulphone also produced respectable CHOP activation compared to **3** (**18–20**). Compound lipophilicity ranged from 0.4–4.6, with no apparent trend in the CHO–CHOP assay, and these analogues did not induce the XBP1 pathway (AC₅₀ > 80 μ M). Several furyl group replacements were explored (blue region of **3**, Figure 1); however, none proved superior to the parent 5-nitrofuryl moiety (**21–26**). Moreover, exchange of the nitro group with a hydrogen atom (**27**), methyl group (**28**), bromine atom (**29**), or a trifluoromethyl group (**30**) all resulted in loss of activity. For this select group of analogues, the 5-nitrofuryl functionality was necessary to retain CHOP activity.

Preliminary data indicated low micromolar (<10 μ M) growth inhibition in several human cancer cell lines exposed to compounds that selectively activated the CHOP reporter (data not shown). A panel of analogues (**10–15**) was subsequently used for proliferation assays with wildtype or *Chop* knockout murine embryonic fibroblast (MEF) cell lines. Although MEFs were not expected to exactly recapitulate any human disease, we hypothesized that wildtype (WT) cells would be more sensitive to CHOP activators, while CHOP null cells would be protected. MEF cell lines were treated in a dose response fashion for 16 h, and proliferation was measured using an ATP-based luminescent assay (Table 2). The ability of compounds **10–15** to inhibit proliferation in *Chop*-null MEF cells was

Table 2. MEF Proliferation Assay Data

compd	CHOP AC ₅₀ ± SEM (μM) ^a	CHOP WT EC ₅₀ ± SEM (μM) ^{b,c}	CHOP KO EC ₅₀ ± SEM (μM) ^{b,c}	cLogP ^d
10	1.2 ± 0.2	7.8 ± 1.2	>20	2.6
11	0.6 ± 0.1	17.5 ± 2.7	>20	2.3
12	0.8 ± 0.04	4.8 ± 1.1	>20	2.7
13	0.7 ± 0.1	4.6 ± 1.2	16.3 ± 1.0	3.1
14	0.6 ± 0.1	3.0 ± 0.6	9.2 ± 3.3	3.6
15	0.7 ± 0.1	1.4 ± 0.5	2.1 ± 0.3	4.4

^aCHO–CHOP–luciferase cells. ^bData were averaged from *n* = 4 experiments performed with triplicate samples. ^cMEF cells. ^dCalculated using CambridgeSoft ChemBioDraw Ultra 12.0.

diminished and appeared to track with changes in lipophilicity, a result that could be due to permeability or transport differences between cell types. Compound **11** was the least lipophilic (cLogP 2.3) and required higher concentrations to reduce proliferation. Compounds **10** and **12** were slightly more lipophilic than **11** and selectively reduced proliferation of the WT MEF cells. In four independent experiments using triplicate samples *Chop*-null MEF cells were unaffected by concentrations up to 20 μ M after 24 h (Figure S1, Supporting Information). Compounds **13–15** were comparatively more lipophilic (cLogP 3.1–4.4) and were among the most potent CHOP-luc cell activators. The fact that **13–15** reduced proliferation in both MEF cell lines suggested that this subset of analogues might utilize a *Chop*-independent mechanism of growth inhibition.

Compound **12** appeared to have a well-balanced profile in terms of cLogP, selectivity for activating the CHO–CHOP–luciferase reporter versus the adaptive XBP1 reporter, and reduced proliferation in a *Chop*-dependent fashion; therefore, this compound was selected for further studies assessing effects on UPR gene expression in human cells. Since our previous work has demonstrated that oral squamous cell carcinoma (OSCC) cell lines are sensitive to UPR-inducing compounds compared to normal, nonmalignant cells, we performed dose–response proliferation assays in a panel of OSCC cells. Cells were treated with increasing concentrations of compound **12** for 24 h. Moderate single-digit micromolar potency was observed in UMSCC-23 (7.3 ± 1.7 μ M), HN12 (7.2 ± 0.7 μ M), and HN30 (9.0 ± 1.1 μ M); whereas A253, H460/T800, and HN6 were more resistant (Figure S2, Supporting Information). There is no obvious common thread we are aware of to explain the differences in sensitivity (e.g., p53 status or TGF β –SMAD signaling defects). To assess the ability of compound **12** to reduce proliferation in a broad range of human cancers, it was screened using the National Cancer Institute’s Developmental Therapeutics Program human tumor cell line panel (NCI-60). Very promising low micromolar potency against colon, melanoma, and renal cancer cell lines was observed (Figure S3 and Table S1, Supporting Information). Considered together, the OSCC and NCI-60 data indicate that compound **12** is not generally cytotoxic across malignancies. Ongoing studies to identify specific molecular signatures that regulate sensitivity will help to identify which cancers/patients might benefit most from compound **12** or its analogues.

Since compound **12** demonstrated promising antitumor activity, we examined the expression of UPR and CHOP target genes in OSCC. UMSCC23 cells were treated with compound **12** in a dose–response fashion for 6 h. Cells were then lysed,

and cDNA pools were generated using random hexamers. Quantitative real-time reverse transcription PCR (qRT-PCR) analysis revealed increased transcripts for *CHOP*, spliced *XBPI*, and *GADD34* (Figure 2). Notably, *CHOP* transcripts were 5-

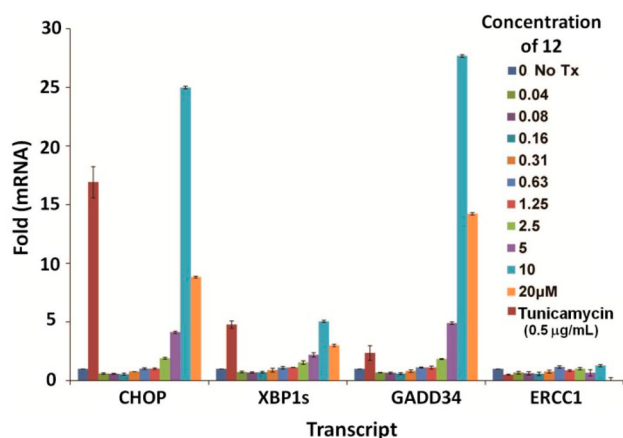


Figure 2. qRT-PCR studies with **12**. Tunicamycin (Tm) was used as a positive control for the induction of ER stress and the UPR.

fold higher than spliced *XBPI* at 10 μ M, indicating selectivity similar to that observed using CHO-UPR-luciferase reporter cells (Table 1). Furthermore, the DNA repair gene *ERCC1* was not increased suggesting compound **12**-induced *CHOP* expression is not a result of DNA-adduct formation and strand breaks. Decreased gene expression for each transcript at 20 μ M coincided with cell death as evidenced by cells lifting off the dish before the end of the experiment. Selective activation of the apoptotic (*CHOP*) arm of the UPR and submicromolar growth inhibition potency in a broad range of human cancer cell lines support the notion that **12** is an appropriate chemical probe for proof-of-concept *in vivo* xenograft studies.

While certain attributes such as aqueous solubility and stability were assessed at an early stage of the project to guide the hit selection process, more advanced *in vitro* pharmacology was examined only for compound **12** in order to establish baseline parameters for future optimization efforts. Chemical stability of **12** was determined by treating **12** (10 μ M in PBS at pH 7.4 with 1% DMSO) separately with a 5-fold excess of thiol nucleophiles, glutathione (GSH) or dithiothreitol (DTT), for 8 h at room temperature. In each case, 100% of **12** remained with no detectable GSH or DTT adducts formed. These results support that the acyl 5-nitro-2-furan was not prone to act as a Michael acceptor.⁴²

A number of ADME parameters were also examined for compound **12** (Table S2, Supporting Information).⁴³ Aqueous stability in PBS and pION buffer through a biologically relevant pH range was determined to be 8.7–9.7 μ M. The solubility was highest at physiological pH 7.4 and registered approximately 13–15-fold over its EC_{50} (0.8 μ M), revealing that its potency was not severely limited by its solubility. A PAMPA assay was used as an *in vitro* model of passive, transcellular permeability. Using UV spectroscopy to evaluate compound concentration between different compartments, compound **12** was determined to have good permeability at pH values of 5.0, 6.2, and 7.4 in the donor compartment, with the highest permeability at pH 6.2. The compound was highly plasma protein bound to human plasma proteins (>99%), though it was somewhat less tightly bound to mouse plasma proteins (~84%). In human

plasma, **12** was moderately stable (~86% remaining), though reduced stability in mouse plasma (52% remaining) was observed. The compound was almost completely metabolized in both human and mouse liver homogenates within 1 h, and some toxicity was also noted toward human hepatocytes (~11 μ M). The promiscuity of compound **12** was also investigated by profiling the analogue at a 10 μ M concentration against a Panlabs LeadProfiling Screen that included a panel of 67 GPCRs, nuclear receptors, transporters, and ion channels.⁴⁴ Significant inhibition, defined as >50% of any single target, was found to be 68% for the human dopamine receptor. Thus, the off-target profile for **12** was determined to be relatively clean, and the significance of dopamine transporter inhibition, though noted, is measured given that modifications to the prototype scaffold will be necessary to advance the compound series.

To further characterize the profile of compound **12**, its bioavailability was assessed in male CD-1 mice by IV (2 mg/kg single dose) and IP (30 mg/kg single dose) administration.⁴⁵ Plasma concentrations were determined at 7 intervals over 8 h for each cohort (3 mice in each group). The IV dose of **12** was readily cleared from circulation within 30 min of administration. Plasma concentrations of **12** following IP administration declined more gradually, although suboptimal exposure was determined throughout the 8 h testing window (C_{max} = 0.14 μ M; T_{max} = 0.17 h). While these initial *in vivo* results clearly suggest that further structural refinement will likely be necessary in order to obtain sufficient exposure in future *in vivo* studies, multiple variables such as metabolic liability, biodistribution, and target identification should be determined to better guide the optimization process.

In conclusion, a screening campaign focused on finding selective inducers of the UPR apoptotic *CHOP* pathway revealed a sulfonamidebenzamide scaffold with single-digit micromolar cellular potency and no liability toward the adaptive, *XBPI* pathway of the UPR. An optimization effort delivered analogues with improved, submicromolar potency that were further characterized in terms of their ability to selectively induce *CHOP* genes at the mRNA level and demonstrated antiproliferative activity in multiple cancer cell lines. Importantly, these outcomes lay the groundwork for more advanced studies that will (1) examine the effects of these compounds in an OSCC xenograft mouse model, (2) attempt to discern the specific target within the *CHOP* pathway with which these compounds interact, and (3) provide more extensive SAR data directed at improving the overall pharmacokinetic profile for downstream *in vivo* efficacy studies.

■ ASSOCIATED CONTENT

● Supporting Information

General chemical methods, experimental and analytical characterization for new intermediates and compounds **3** and **7–30**, cell assay protocols, *in vitro* pharmacology assay protocols, full NCI-60 panel results, and off-target PanLabs profiling results and methods. This material is available free of charge via the Internet at <http://pubs.acs.org>.

■ AUTHOR INFORMATION

Corresponding Authors

*(J.E.G.) E-mail: jengolden@ku.edu.

*(A.M.F.) E-mail: afribley@med.wayne.edu.

*(R.J.K.) E-mail: rkaufman@sanforburnham.org.

Funding

The authors gratefully acknowledge funding from the following sources. Chemistry efforts at the University of Kansas Specialized Chemistry Center were supported by NIH U54HG005031 to J.A. KU NMR instrumentation was supported by NIH S10RR024664 and NSF 0320648. High throughput screening performed at the Conrad Prebys Center for Chemical Genomics at the Sanford Burnham Medical Research Institute was supported by NIH U54 HG00503. R.J.K. acknowledges support from R03MH089782-01, DK042394, DK088227, and HL052173. A.F. was supported by DE019678 and the Wayne State University Fund for Medical Research. Portions of this work were supported by shared resources from the NCI Cancer Center grant 5P30CA030199.

Notes

The authors declare no competing financial interest.

■ ABBREVIATIONS

ATF4, activating transcription factor 4; CHO, Chinese hamster ovary; CHOP, C/EBP-homologous protein; DTT, dithiothreitol; ER, endoplasmic reticulum; ERCC1, excision repair cross-complementation group 1; GADD34, growth and DNA damage 34; GSH, glutathione; HTS, high throughput screen; IP, intraperitoneal; IV, intravenous; KO, knockout; MEF, murine embryonic fibroblast; OSCC, oral squamous cell carcinoma; PAMPA, parallel artificial membrane permeability assay; PCR, polymerase chain reaction; SAR, structure–activity relationship; UPR, unfolded protein response; UV, ultraviolet; WT, wildtype; XBP1, X-box binding protein 1

■ REFERENCES

- (1) Rutkowski, D. T.; Kaufman, R. J. A trip to the ER: coping with stress. *Trends Cell Biol.* **2004**, *14*, 20–28.
- (2) Schröder, M.; Kaufman, R. J. The mammalian unfolded protein response. *Annu. Rev. Biochem.* **2005**, *74*, 739–789.
- (3) Kaufman, R. J. Stress signaling from the lumen of the endoplasmic reticulum: coordination of gene transcriptional and translational controls. *Genes Dev.* **1999**, *13*, 1211–1233.
- (4) Bernales, S.; Papa, F. R.; Walter, P. Intracellular signaling by the unfolded protein response. *Annu. Rev. Cell Dev. Biol.* **2006**, *22*, 487–508.
- (5) Calton, M.; Zeng, H.; Urano, F.; Till, J. H.; Hubbard, S. R.; Harding, H. P.; Clark, S. G.; Ron, D. IRE1 couples endoplasmic reticulum load to secretory capacity by processing the XBP-1 mRNA. *Nature* **2002**, *415*, 92–96.
- (6) Acosta-Alvear, D.; Zhou, Y.; Blais, A.; Tsikitis, M.; Lents, N. H.; Arias, C.; Lennon, C. J.; Kluger, Y.; Dynlacht, B. D. XBP1 controls diverse cell type- and condition-specific transcriptional regulatory networks. *Mol. Cell* **2007**, *27*, 53–66.
- (7) Hetz, C. The unfolded protein response: controlling cell fate decisions under ER stress and beyond. *Nat. Rev. Mol. Cell Biol.* **2012**, *13*, 89–102.
- (8) Marciniak, S. J.; Yun, C. Y.; Oyadomari, S.; Novoa, I.; Zhang, Y.; Jungreis, R.; Nagata, K.; Harding, H. P.; Ron, D. CHOP induces death by promoting protein synthesis and oxidation in the stressed endoplasmic reticulum. *Genes Dev.* **2004**, *18*, 3066–3077.
- (9) Matsumoto, M.; Minami, M.; Takeda, K.; Sakao, Y.; Akira, S. Ectopic expression of CHOP (GADD153) induces apoptosis in M1 myeloblastic leukemia cells. *FEBS Lett.* **1996**, *395*, 143–147.
- (10) Oyadomari, S.; Mori, M. Roles of CHOP/GADD153 in endoplasmic reticulum stress. *Cell Death Differ.* **2003**, *11*, 381–389.
- (11) Han, J.; Back, S. H.; Hur, J.; Lin, Y.-H.; Gildersleeve, R.; Shan, J.; Yuan, C. L.; Krokowski, D.; Wang, S.; Hatzoglou, M.; Kilberg, M. S.; Sartor, M. A.; Kaufman, R. J. ER-stress-induced transcriptional

regulation increases protein synthesis leading to cell death. *Nat. Cell Biol.* **2013**, *15*, 481–490.

- (12) Nakagawa, H.; Umemura, A.; Taniguchi, K.; Font-Burgada, J.; Dhar, D.; Ogata, H.; Zhong, Z.; Valasek, M. A.; Seki, E.; Hidalgo, J.; Koike, K.; Kaufman, R. J.; Karin, M. ER stress cooperates with hypernutrition to trigger TNF-dependent spontaneous HCC development. *Cancer Cell* **2014**, *26*, 331–343.

- (13) Roussel, B. D.; Kruppa, A. J.; Miranda, E.; Crowther, D. C.; Lomas, D. A.; Marciniak, S. J. Endoplasmic reticulum dysfunction in neurological disease. *Lancet Neurol.* **2013**, *12*, 105–118.

- (14) Kaser, A.; Flak, M. B.; Tomczak, M. F.; Blumberg, R. S. The unfolded protein response and its role in intestinal homeostasis and inflammation. *Exp. Cell Res.* **2011**, *317*, 2772–2779.

- (15) Cao, S. S.; Kaufman, R. J. Targeting endoplasmic reticulum stress in metabolic disease. *Expert Opin. Ther. Targets* **2013**, *17*, 437–448.

- (16) Scheuner, D.; Kaufman, R. J. The unfolded protein response: a pathway that links insulin demand with β -cell failure and diabetes. *Endocr. Rev.* **2008**, *29*, 317–333.

- (17) Moenner, M.; Pluquet, O.; Bouche-careilh, M.; Chevet, E. Integrated endoplasmic reticulum stress responses in cancer. *Cancer Res.* **2007**, *67*, 10631–10634.

- (18) Cross, B. C.; Bond, P. J.; Sadowski, P. G.; Jha, B. K.; Zak, J.; Goodman, J. M.; Silverman, R. H.; Neubert, T. A.; Baxendale, I. R.; Ron, D. The molecular basis for selective inhibition of unconventional mRNA splicing by an IRE1-binding small molecule. *Proc. Natl. Acad. Sci. U.S.A.* **2012**, *109*, E869–E878.

- (19) Papandreou, I.; Denko, N. C.; Olson, M.; Van Melckebeke, H.; Lust, S.; Tam, A.; Solow-Cordero, D. E.; Bouley, D. M.; Offner, F.; Niwa, M. Identification of an Ire1 α endonuclease specific inhibitor with cytotoxic activity against human multiple myeloma. *Blood* **2011**, *117*, 1311–1314.

- (20) Axten, J. M.; Medina, J. S. R.; Feng, Y.; Shu, A.; Romeril, S. P.; Grant, S. W.; Li, W. H. H.; Heering, D. A.; Minthorn, E.; Mencken, T. Discovery of 7-methyl-5-(1-([3-(trifluoromethyl) phenyl] acetyl)-2,3-dihydro-1H-indol-5-yl)-7H-pyrrolo[2,3-d]pyrimidin-4-amine (GSK2606414), a potent and selective first-in-class inhibitor of protein kinase R (PKR)-like endoplasmic reticulum kinase (PERK). *J. Med. Chem.* **2012**, *55*, 7193–7207.

- (21) D'Arcy, P.; Brnjic, S.; Olofsson, M. H.; Fryknäs, M.; Lindsten, K.; De Cesare, M.; Perego, P.; Sadeghi, B.; Hassan, M.; Larsson, R. Inhibition of proteasome deubiquitinating activity as a new cancer therapy. *Nat. Med.* **2011**, *17*, 1636–1640.

- (22) Boyce, M.; Bryant, K. F.; Jousse, C.; Long, K.; Harding, H. P.; Scheuner, D.; Kaufman, R. J.; Ma, D.; Coen, D. M.; Ron, D. A selective inhibitor of eIF2 α dephosphorylation protects cells from ER stress. *Science* **2005**, *307*, 935–939.

- (23) Fribley, A. M.; Cruz, P. G.; Miller, J. R.; Callaghan, M. U.; Cai, P.; Narula, N.; Neubig, R. R.; Showalter, H. D.; Larsen, S. D.; Kirchhoff, P. D.; Larsen, M. J.; Burr, D. A.; Schultz, P. J.; Jacobs, R. R.; Tamayo-Castillo, G.; Ron, D.; Sherman, D. H.; Kaufman, R. J. Complementary cell-based high-throughput screens identify novel modulators of the unfolded protein response. *J. Biomol. Screening* **2011**, *16*, 825–835.

- (24) Hetz, C.; Chevet, E.; Harding, H. P. Targeting the unfolded protein response in disease. *Nat. Rev. Drug Discovery* **2013**, *12*, 703–719.

- (25) Wilhelm, S. M.; Adnane, L.; Newell, P.; Villanueva, A.; Llovet, J. M.; Lynch, M. Preclinical overview of sorafenib, a multikinase inhibitor that targets both Raf and VEGF and PDGF receptor tyrosine kinase signaling. *Mol. Cancer Ther.* **2008**, *7*, 3129–3140.

- (26) Smalley, K. S.; Xiao, M.; Villanueva, J.; Nguyen, T. K.; Flaherty, K. T.; Letrero, R.; Van Belle, P.; Elder, D. E.; Wang, Y.; Nathanson, K. L.; Herlyn, M. CRAF inhibition induces apoptosis in melanoma cells with non-V600E BRAF mutations. *Oncogene* **2009**, *28*, 85–94.

- (27) Magnaghi, P.; D'Alessio, R.; Valsasina, B.; Avanzi, N.; Rizzi, S.; Asa, D.; Gasparri, F.; Cozzi, L.; Cucchi, U.; Orrenius, C.; Polucci, P.; Ballinari, D.; Perrera, C.; Leone, A.; Cervi, G.; Casale, E.; Xiao, Y.; Wong, C.; Anderson, D. J.; Galvani, A.; Donati, D.; O'Brien, T.;

Jackson, P. K.; Isacchi, A. Covalent and allosteric inhibitors of the ATPase VCP/p97 induce cancer cell death. *Nat. Chem. Biol.* **2013**, *9*, 548–556.

(28) Brem, G. J.; Mylonas, I.; Bruning, A. Eeyarestatin causes cervical cancer cell sensitization to bortezomib treatment by augmenting ER stress and CHOP expression. *Gynecol. Oncol.* **2013**, *128*, 383–90.

(29) Chou, T. F.; Brown, S. J.; Minond, D.; Nordin, B. E.; Li, K.; Jones, A. C.; Chase, P.; Porubsky, P. R.; Stoltz, B. M.; Schoenen, F. J.; Patricelli, M. P.; Hodder, P.; Rosen, H.; Deshaies, R. J. Reversible inhibitor of p97, DBeQ, impairs both ubiquitin-dependent and autophagic protein clearance pathways. *Proc. Natl. Acad. Sci. U.S.A.* **2011**, *108*, 4834–4839.

(30) Jhaveri, K.; Taldone, T.; Modi, S.; Chiosis, G. Advances in the clinical development of heat shock protein 90 (Hsp90) inhibitors in cancers. *Biochim. Biophys. Acta* **2012**, *1823*, 742–755.

(31) Adams, J.; Kauffman, M. Development of the proteasome inhibitor velcade (bortezomib). *Cancer Invest.* **2004**, *22*, 304–311.

(32) Kisselev, A. F.; van der Linden, W. A.; Overkleeft, H. S. Proteasome inhibitors: an expanding army attacking a unique target. *Chem. Biol.* **2012**, *19*, 99–115.

(33) Fribley, A.; Zeng, Q.; Wang, C.-Y. Proteasome inhibitor PS-341 induces apoptosis through induction of endoplasmic reticulum stress-reactive oxygen species in head and neck squamous cell carcinoma cells. *Mol. Cell. Biol.* **2004**, *24*, 9695–9704.

(34) Fribley, A. M.; Evenchik, B.; Zeng, Q.; Park, B. K.; Guan, J. Y.; Zhang, H.; Hale, T. J.; Soengas, M. S.; Kaufman, R. J.; Wang, C. Y. Proteasome inhibitor PS-341 induces apoptosis in cisplatin-resistant squamous cell carcinoma cells by induction of Noxa. *J. Biol. Chem.* **2006**, *281*, 31440–31447.

(35) Mitsiades, N.; Mitsiades, C. S.; Poulaki, V.; Chauhan, D.; Fanourakis, G.; Gu, X.; Bailey, C.; Joseph, M.; Libermann, T. A.; Treon, S. P.; Munshi, N. C.; Richardson, P. G.; Hideshima, T.; Anderson, K. C. Molecular sequelae of proteasome inhibition in human multiple myeloma cells. *Proc. Natl. Acad. Sci. U.S.A.* **2002**, *99*, 14374–14379.

(36) Leung-Hageteijn, C.; Erdmann, N.; Cheung, G.; Keats, J. J.; Stewart, A. K.; Reece, D. E.; Chung, K. C.; Tiedemann, R. E. Xbp1s-negative tumor B cells and pre-plasmablasts mediate therapeutic proteasome inhibitor resistance in multiple myeloma. *Cancer Cell* **2013**, *24*, 289–304.

(37) Fribley, A. M.; Miller, J. R.; Brownell, A. L.; Garshott, D. M.; Zeng, Q.; Reist, T. E.; Narula, N.; Cai, P.; Xi, Y.; Callaghan, M. U.; Kodali, V.; Kaufman, R. J. Celastrol induces unfolded protein response-dependent cell death in head and neck cancer. *Exp. Cell Res.* **2014**, DOI: 10.1016/j.yexcr.2014.08.014.

(38) See PubChem Summary AID: 4497771. For CHO-CHOP assay, see AID602434. For XBP1 assay, see AID602416.

(39) Harding, H. P.; Zhang, Y.; Khersonsky, S.; Marciniak, S.; Scheuner, D.; Kaufman, R. J.; Javitt, N.; Chang, Y.-T.; Ron, D. Bioactive small molecules reveal antagonism between the integrated stress response and sterol-regulated gene expression. *Cell Metab.* **2005**, *2*, 361–371.

(40) Back, S. H.; Lee, K.; Vink, E.; Kaufman, R. J. Cytoplasmic IRE1 α -mediated XBP1 mRNA splicing in the absence of nuclear processing and endoplasmic reticulum stress. *J. Biol. Chem.* **2006**, *281*, 18691–18706.

(41) Hayashi, S.; Nakamoto, T.; Minoura, M.; Nakanishi, W. Evidence for effective p(Z)– π (Ar) conjugations (Z = S, Se, and Te, as well as Z = O) in 9-(arylchalcogenyl)tritylenes: experimental and theoretical investigations. *J. Org. Chem.* **2009**, *74*, 4763–4771.

(42) Chemical stability studies performed by Mr. Patrick Porubsky, University of Kansas Specialized Chemistry Center Analytical Core.

(43) *In vitro* ADME studies performed by Ms. Arianna Mangravita-Novo and Mr. Michael Vicchiarelli of the Conrad Prebys Center for Chemical Genomics at the Sanford Burnham Medical Institute Exploratory Pharmacology Analysis Laboratory at Lake Nona, FL under the direction of Dr. Layton H. Smith.

(44) Formerly Ricerca Biosciences; see Table S3, Supporting Information.

(45) *In vivo* experiments were performed by WuXi AppTec via the Conrad Prebys Center for Chemical Genomics.